



23rd International Conference on Material Forming (ESAFORM 2020)

# Material Modeling in Forming Simulation of Three-Dimensional Fiber-Metal-Laminates – A Parametric Study

Henrik Oliver Werner<sup>a,b,\*</sup>, Christian Poppe<sup>a</sup>, Frank Henning<sup>a,c</sup>, Luise Kärger<sup>a</sup>

<sup>a</sup>Karlsruhe Institute of Technology (KIT), Institute of Vehicle System Technology, Rintheimer Querallee 2, 76131 Karlsruhe, Germany

<sup>b</sup>Karlsruhe Institute of Technology (KIT), Institute for Applied Materials, Engelbert-Arnold-Straße 4, 76131 Karlsruhe, Germany

<sup>c</sup>Fraunhofer Institute for Chemical Technology, Polymer Engineering Department, Joseph-von-Fraunhofer-Str. 7, 76327 Pfanzelt, Germany

\* Corresponding author. Tel.: +49-721-608-41877; fax: +49-721-608-48044. E-mail address: [henrik.werner@kit.edu](mailto:henrik.werner@kit.edu)

## Abstract

Forming of fiber-metal-laminates (FML) into complex geometries is challenging, due to the low fracture toughness of the fibers. Several researchers have addressed this topic in recent years. A new manufacturing process has been introduced in our previous work that successfully combines deep drawing with thermoplastic resin transfer molding (T-RTM) in a single process step. During molding, the fabric is infiltrated with a reactive monomeric matrix, which polymerizes to a thermoplastic after the forming process is completed. In our previous work, a numerical modeling approach was presented for this fully integrated process, investigating a hybrid laminate with 1 mm thick metal sheets of DC04 as top layers and three inner glass fiber layers. Although initial results were promising, there were still some pending issues regarding the modeling of material behavior. The current study aims to address several of these open issues and to provide a general modelling framework for future enhancements. For this purpose, the existing modelling approach is extended and used for parameter analysis. Regarding the influence of different material characteristics on the forming result, shear, bending and compression properties of the fabric are modified systematically. It is shown, that the compression behavior and particularly the tension-compression anisotropy of the fabric is of high importance for modelling the combined forming of fabric and metal. The bending and shear properties of the fabric are negligible small compared to the metal stiffness which dominates the draping process. Finally, it is demonstrated that modelling the fabric layers using continuum shells provides a promising approach for future research, as it enables a suitable way to account for transversal compaction during molding.

© 2020 The Authors. Published by Elsevier Ltd.

This is an open access article under the CC BY-NC-ND license (<https://creativecommons.org/licenses/by-nc-nd/4.0/>)  
Peer-review under responsibility of the scientific committee of the 23rd International Conference on Material Forming.

*Keywords:* Process simulation; FE-Forming Simulation; Fiber-Metal-Laminates; Hybrid; T-RTM; RTM; deep drawing

## 1. Introduction

Fiber metal laminates (FML) belong to the group of material composites and consist of alternating thin layers of metal sheets and fiber composite layers (FRP). This hybrid material class was developed for the aviation industry in the 1980s [1], with a scope on very high resistance to crack propagation and good impact properties. It is possible to adapt the material properties of the hybrid composite exactly to the required profile, by selection of metal sheet, fiber and matrix material, its fiber orientation, as well as the respective layer thicknesses and sequences. This customizability makes FML promising beyond

the aerospace industry. However, the conventional production process used so far, involving individual deposition of the respective layer and curing in an autoclave, is complex and expensive [2]. In addition, the design freedom for the constructing engineer is severely restricted by the manufacturing process with regard to the geometric shape. Geometries with multiple curvatures and small radii of curvature are not feasible. The post-processing of FML using traditional machining processes, such as milling, is also difficult and only possible to a limited extent [3].

In order for the FML to become interesting for other industries or applications, the manufacturing costs have to be

2351-9789 © 2020 The Authors. Published by Elsevier Ltd.

This is an open access article under the CC BY-NC-ND license (<https://creativecommons.org/licenses/by-nc-nd/4.0/>)  
Peer-review under responsibility of the scientific committee of the 23rd International Conference on Material Forming.  
10.1016/j.promfg.2020.04.160

reduced and the geometric complexity of the producible FML has to increase. Deep drawing is a common, widely applied and inexpensive process in sheet metal processing for the production of large quantities. It also allows high degrees of sheet metal forming and complex geometries curved in several directions. In recent years, various research groups have been working on making this process usable for the production of FML [4 - 11]. They encountered a number of challenges. Metal sheets and fibers can buckle if blank holder forces are not sufficient [5, 6]. If the blank holder force is too high, the metal sheets and fibers will tear [7]. In zones of low external pressure, matrix accumulations occur [8], since prepregs or pre-consolidated thermoplastic semi-finished fiber products are usually used for FRP. The prepregs and pre-consolidated thermoplastic fiber semi-finished products have a predefined fiber volume content. The high viscosity of the matrix leads to high internal pressures between two metal layers and thus to matrix accumulations in zones of low external pressure. Another challenge is the adhesion between metal sheet and FRP. If the adhesion is too low, delamination and gapping will occur [9], which significantly reduces final part performance.

We introduced a new manufacturing process for FML in our previous work [10]. It combines deep drawing with thermoplastic resin transfer molding (T-RTM). The fabric is infiltrated with a reactive monomeric matrix during forming, which polymerizes to a thermoplastic after completion of the forming process, as shown in Fig. 1. The matrix also creates the interface to the metal sheets. This prevents matrix accumulations and delaminations in the final part. However, the blank holder force has been chosen carefully, as too high blank holder forces in this process also increases the infiltration resistance.

For the integrated process, we presented a numerical modeling approach in our previous work [11]. Fluid propagation is neglected in this approach due to the already high complexity of the process. The metal sheets of DC04 and the E-glass fiber layers are represented by shell elements,

which means that transverse compaction behavior is neglected. A double symmetric model as shown in Fig. 2 was used.

A large influence of the metal sheets on the forming of the textile was found. Strong shear bands were predicted by the initial simulation approach within the textile. The orientation of the shear bands corresponds to the direction of fiber draw-in. Unfortunately, experimental results do not show this effect, as illustrated in Fig. 3. Regarding the predicted shear bands, a numerical effect is assumed to be the source, which results from the modeling of the in-plane compression of the fabric. This is addressed first within this study. Regarding model assumptions, the influence of symmetry, fiber orientation and blank holder force is investigated. In addition, the influence of the material parameters of the textile model (shear, compression and bending properties) are investigated.

Consequently, this parameter study aims to provide the individual sensitivities of the material parameters and modeling approaches within the process. By this means, important effects and material parameters can be identified and investigated in more detail in further studies, whereas insignificant parameters can be neglected in future investigations.

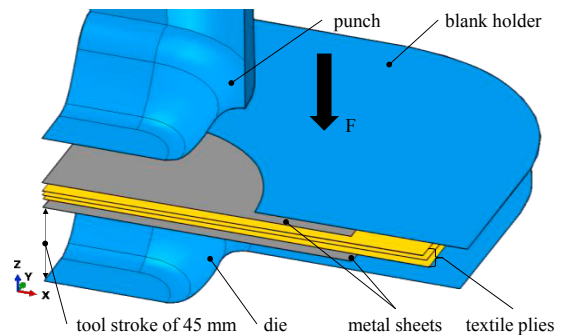


Fig. 2. Simulation model with double symmetric boundary conditions.

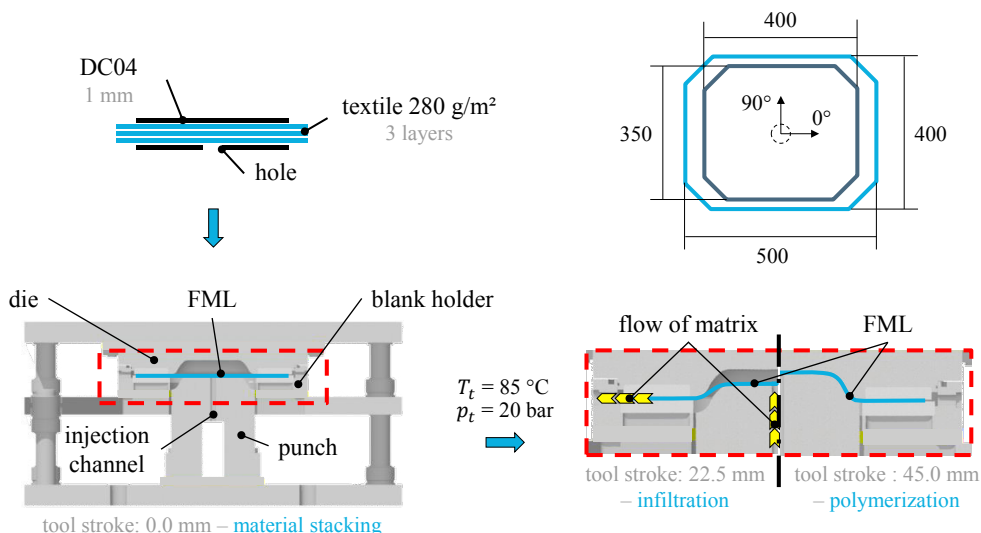


Fig. 1. Process flow of combined deep drawing and injection process.

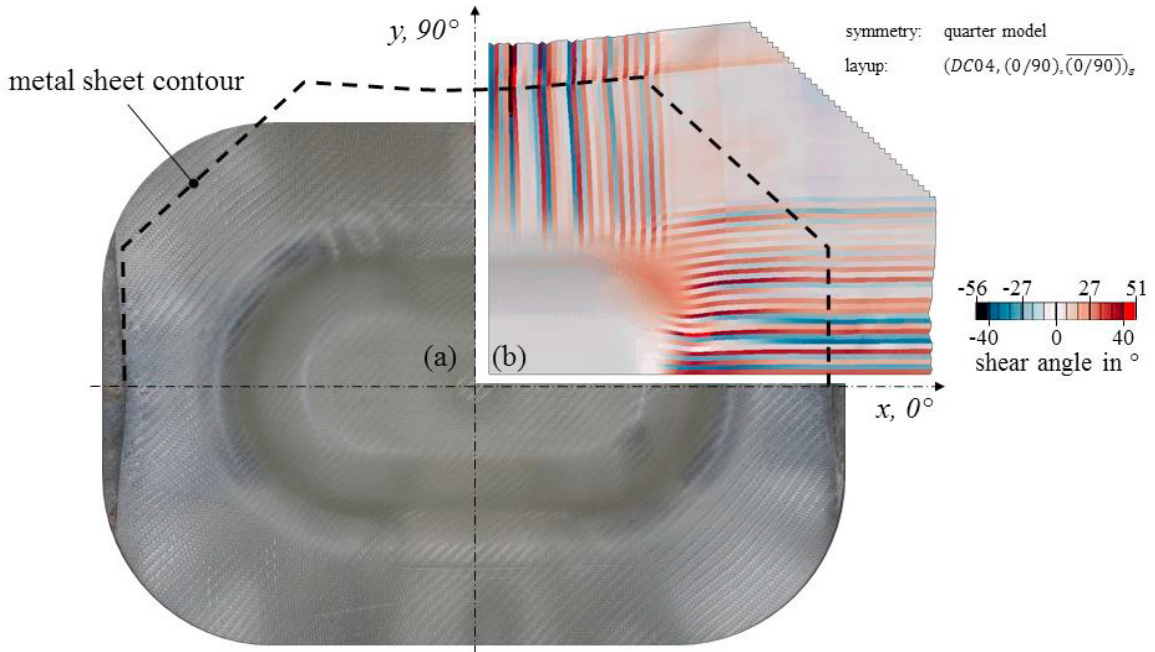


Fig. 3. (a) Experimental forming result with removed metal sheets; (b) Result from previous process modelling study with massive shear bands [11].

## 2. Modelling of the deep drawing process

The process simulation is performed in the multi-purpose finite element solver ABAQUS/EXPLICIT, based on an existing forming simulation framework developed at KIT-FAST [12, 13]. The tool geometry is modeled as a rigid, discrete surface, because the expected tool deformation is negligible compared to the deformation of the part. Contact is modeled by means of the ABAQUS built-in general contact algorithm. Tool-ply and ply-ply interface behavior is modeled by normal contact stiffness and frictional behavior in tangential direction. The drawing depth is 45 mm and smooth amplitudes are used for the displacement-controlled tool stroke. Prior to the onset of the tool stroke, a blank holder force is applied to the double-symmetric model. Only a quarter of the double-symmetric component is modeled in ABAQUS (Fig. 2). A quarter model contains 156764 elements. In the initial configuration, the fiber orientation is parallel to the short edges of the equilateral triangles. Two reference configurations are modeled without symmetry boundary conditions (BC) as full models to check, if the symmetry BCs have an influence on the observed shear bands. Material parameters are summarized in Table 1. All interfacial friction values were determined experimentally in accordance with DIN EN ISO 8295 with the test setup and method described in [14].

Table 1. Constant parameters of process simulation.

Model parameter	Constant	Value
Normal contact stiffness	$c_n$	1000 MPa
Tool – metal sheet friction	$\mu_{t,m}$	0.1
Metal sheet – fabric friction	$\mu_{m,f}$	0.25
Fabric – fabric friction	$\mu_{f,f}$	0.334

### 2.1. Blank holder force

The required blank holder force (160 kN) was determined experimentally and is subsequently used as a reference. Lower forces showed wrinkling in the metal sheets and higher blank holder forces produced fracture of the metal sheets and the fabric. Within the parametric study, lower (40 kN) and upper (640 kN) limits are tested for the blank holder force. Forces are scaled accordingly within the quarter models.

### 2.2. Modelling approach for the fabric

To describe the textile behavior, membrane and bending properties have to be decoupled. Therefore, two structural elements are stacked, M3D3 and S3R elements. The M3D3 elements account for the membrane behavior governed by the ABAQUS built-in FABRIC model. It independently calculates the tensile and compressive strains in both fiber directions. The shear behavior is also calculated independently of the two fiber direction strains. Its formulation makes it suitable to account for large strains under consideration of fiber reorientation. Tensile, compression and shear behavior are interpolated from the table data provided by the user. The tensile stiffness is kept constant throughout all simulations and the compression stiffness is varied in three stages (Table 2). As reference, a stiffness of 1.3 MPa is used.

Table 2. FABRIC tensile and compression stiffness.

Model parameter	Constant	Value in MPa
Tensile stiffness	$E_{t,11} = E_{t,22}$	1300.0
Compression stiffness	$E_{c,11} = E_{c,22}$	0.13, <b>1.3</b> , 13.0

The shear stress - shear angle data for the FABRIC model are calculated from a picture frame test with the equations provided by ABAQUS. This is very important, because the FABRIC model uses the initial, not rotating coordinate system instead of the common rotating picture frame coordinate system. The experimental measured shear stress - shear angle curve is used as reference. To test the model's sensitivity to shear input data, the reference curve is multiplied by factor 10 and 100. All three shear stress - shear angle curves are provided in Fig. 4. The increase in shear stress (shear locking) for a defined shear angle can also be found in experimental test data, when picture frame tests with transverse compression forces are performed.

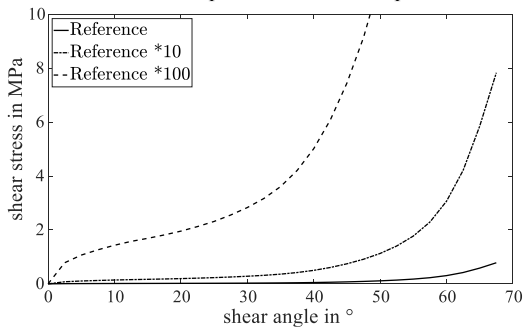


Fig. 4. Shear stress – angle input data for FABRIC model.

Bending properties are represented by a S3R elements with bending idealization for section integration and elastic properties. The bending stiffness is varied in three stages as well, corresponding to Table 3. The reference value is a bending stiffness of 100 MPa. This corresponds to the magnitude usually experimentally determined by cantilever beam tests for this material.

Table 3. Bending stiffness of fabric model.

Model parameter	Constant	Value in MPa
Bending stiffness	$E_{b,11} = E_{b,22}$	10, <b>100</b> , 1000

### 2.3. Metal material

An elastic-plastic material model with isotropic hardening is applied to model the steel sheets. The DC04 steel face sheets are represented by S3R shell elements. For this study, no damage initiation criterion is used, as this provides a significant source of instability and additional complexity to the model. The flow stress curve is shown in Fig. 5.

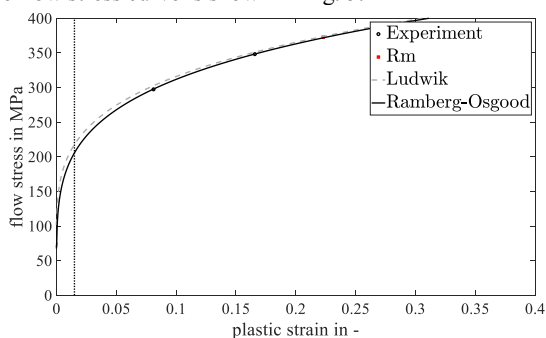


Fig. 5. Flow stress – plastic strain curve of DC04 metal sheet.

## 3. Results

The depicted results in Fig. 6 show the shear angle of reference models without symmetry BCs and reference models with symmetry BCs for layups with  $0^\circ/90^\circ$  and  $\pm 45^\circ$  fiber orientation. The results show no shear locking at the symmetry planes, which is in contrast to the results in our previous study in Fig. 3, where the fabric's compression stiffness was set equal to the fabric's tensile stiffness.

### 3.1. Influence of the symmetry boundary condition

The depicted results in Fig. 6 show a slight influence on the shear angle for the layup with  $0^\circ/90^\circ$  fiber orientation at the symmetry planes. While no shear bands are formed at the symmetry planes in the full model (Fig. 6a), one can see slight shear locking at the symmetry planes for the quarter model (Fig. 6c). The overall shear angle results are not affected by this effect and the shear angles close to the symmetry planes should not be considered in further evaluation. For the layup with  $\pm 45^\circ$  fiber orientation, no influence of the symmetry conditions on the shear angle can be observed (Fig. 6d).

### 3.2. Influence of the fabric properties

In Fig. 7c and Fig. 7d the fabric compression stiffness is varied compared to the reference configuration in Fig. 6c. A decrease of factor 10 of the fabric compression stiffness reduces the shear angle of the fabric at the metal contour in x- and y-direction, because in this directions the fiber is drawn-in. In addition, the shear angles at the symmetry planes are reduced. The general maximal shear angle at the cup geometry is not influenced by the decrease of the fabric compression shear stiffness. An increase of factor 10 of the fabric compression shear stiffness leads to shear bands at the yz-symmetry plane. Due to the formation of shear bands, the increased shear stiffness in relation to the bending stiffness leads to wrinkles (Fig. 7d).

In Fig. 7a and Fig. 7b the fabric bending stiffness is varied compared to the reference configuration in Fig. 6c. A decrease of the bending stiffness leads to wrinkles and an increase reduces the wrinkles.

With increasing shear stiffness by factor 10 (Fig. 8a) and factor 100 (Fig. 8b) the wrinkling of the fabric increases. The shear band formation is decreased with increasing shear stiffness.

### 3.3. Influence of the blank holder force

In Fig. 8c and Fig. 8d the blank holder force is varied. A decrease in the blank holder force from 40 kN in the double symmetric model to 10 kN induces more shear bands compared to the reference configuration in Fig. 6c. The fiber drawn-in is larger with a decreasing blank holder force and thus, leads to larger shear deformation.

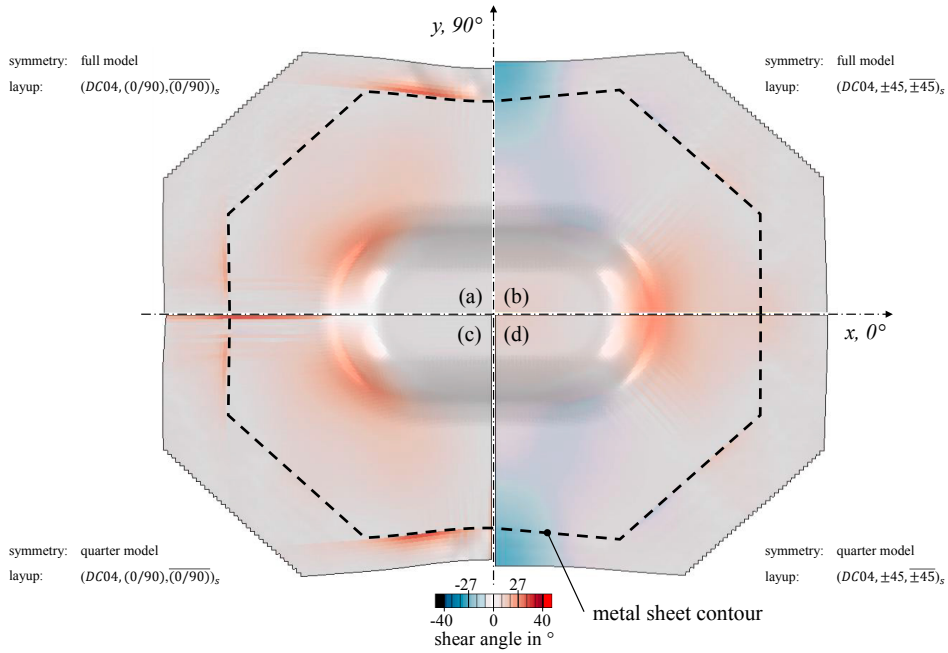


Fig. 6. (a) and (b) shear angle of middle fabric ply for model with no symmetry boundary conditions; (c) and (d) shear angle of middle fabric ply for model with two symmetry planes.

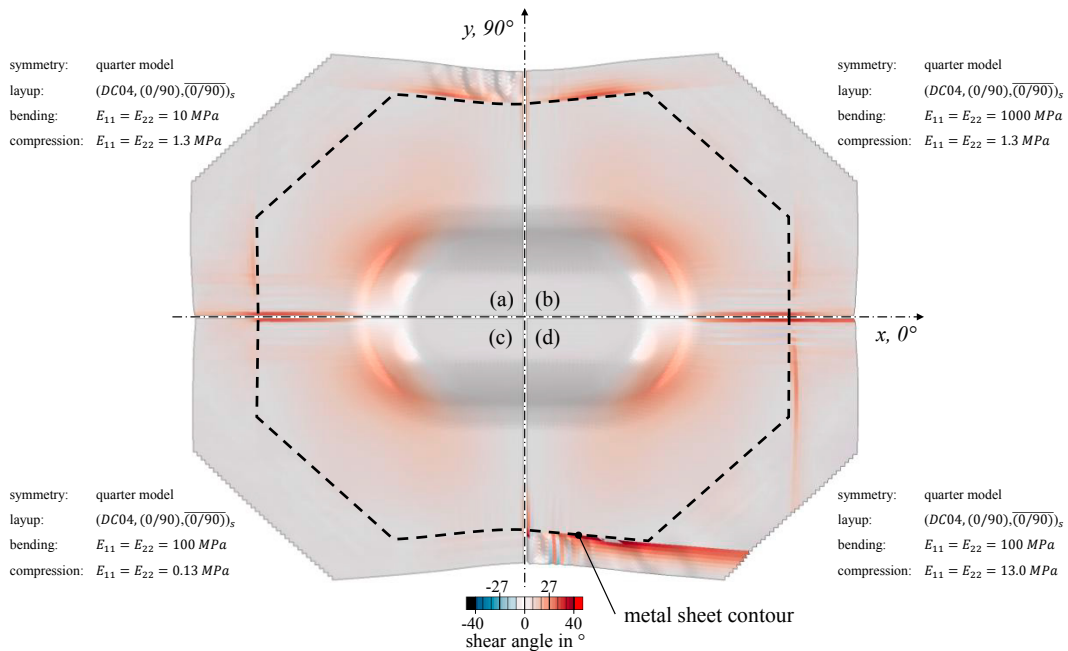


Fig. 7. Shear angles for layups with  $0^\circ/90^\circ$  fiber orientation; (a) and (b) fabric bending stiffness variation; (c) and (d) fabric compression stiffness variation.

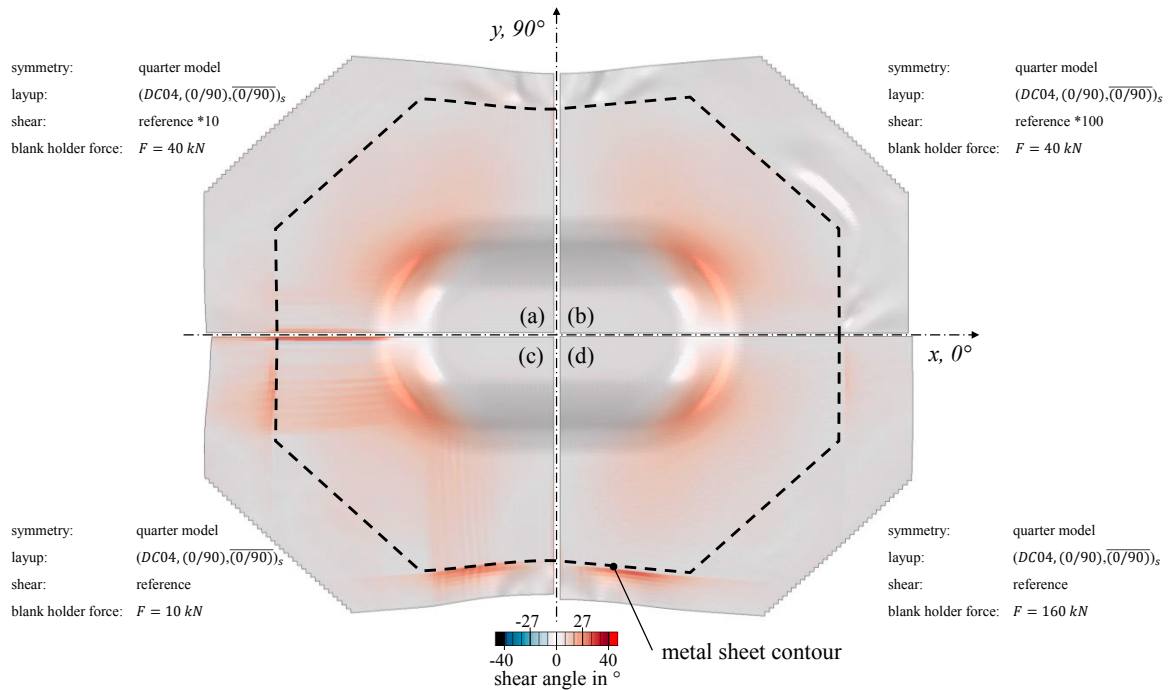


Fig. 8. Shear angles for layups with 0°/90° fiber orientation; (a) and (b) fabric shear stiffness variation; (c) and (d) blank holder force variation.

4. Discussion

The conducted parameter study proves that the previously obtained numerical induced shear band formation results from usage of unsuitable high fabric compression stiffness. Furthermore, the predicted results are governed by a complex interaction of the individual material behavior, such as bending, compression and shear stiffness.

The fabric deforms in the energetically most favorable deformation mode. Table 4 shows the calculated stiffness ratios of the investigated models. The shear stiffness is evaluated at a shear angle of 20°. The results in Fig. 7b and Fig. 7c show no wrinkling of the fabric. They have the highest bending to compression stiffness ratio. The shear bands are reduced in Fig. 7c compared to Fig. 7b, because the compression to shear stiffness ratio in Fig. 7c is lower. This means, to form a shear deformation under compressive strains needs more energy. Fig. 7d shows the strongest shear band formations, because it has the highest compression to shear stiffness ratio.

Table 4. Ratio between bending, compression and shear stiffness of the models. b := bending in MPa, c := compression in MPa, s := shear in MPa°

Model	b/s ratio in °	c/s ratio in °	b/c ratio in -	deformation mode tendency
Fig. 6				
Fig. 8c, d	<b>53.87</b>	<b>0.70</b>	<b>76.92</b>	-
Fig. 7a	5.39	0.70	7.69	wrinkling
Fig. 7b	538.68	0.70	769.23	-
Fig. 7c	53.87	0.07	769.23	-
Fig. 7d	53.87	7.00	7.69	shear bands, wrinkling
Fig. 8a	5.39	0.07	76.92	wrinkling
Fig. 8b	0.54	-0.01	76.92	wrinkling

The ratio of the stiffnesses is decisive for the correct deformation behavior, not the exact stiffness values. Of course, this only applies to the deformation mechanisms, not to the forces and resulting stresses. Furthermore, it has to be noted that the metal sheet dominates the FML forming process. Thus, the fabric draping is kinematically dominated by the metal forming.

5. Frist approach using continuum shell elements

As outlined, versatile effects are to be captured by the applied simulation approach in a suitable manner. However, deformation behavior of the fabric is strongly constrained by the metal sheets during forming. Experimental trials prove local changes of the fabrics' thickness during forming, especially because of the kinematic constrains originating from the metal sheets. Hence, the hitherto prosecuted simulation approach using conventional shell elements with superimposed membrane elements, which implies a predefined constant thickness, is to be questioned.

One particular, more straightforward way to account for local change of thickness during forming is given by the usage of continuum shell (CS) elements. Although they cannot account for a decoupled constitutive description of membrane and bending behavior, they provide the possibility to expand in-plane material behavior, which is currently accounted for by the FABRIC model, to a three-dimensional formulation by introducing a constant thickness modulus. As outlined above, the bending stiffness of the fabric is significantly lower than the bending stiffness of the metal sheets. Therefore, a decoupled modeling for the fabric is not necessary in this case because the metal sheets determine the bending behavior. Moreover, prior studies show that a modification of the transverse shear stiffness values can be utilized to reduce the beforehand

overestimated bending stiffness based on the FABRIC model. Thus, comparable bending properties for the fabric can be reached, without a proper decoupling being accounted for.

To assess the applicability of the approach, the above outlined conventional shell based simulation approach is extended to a three-dimensional formulation by means of CS-elements for all plies in ABAQUS/EXPLICIT using the additional parameters given in Table 5. To ensure comparability with the hitherto applied simulation approach, material and numerical parameters are kept constant wherever possible.

In this manner, the parametrized FABRIC model is applied as before. The same applies to the interaction properties, the metal sheet model and overall tool configuration (c.f. Fig. 2). To account for compaction, a constant thickness modulus  $E_{33}$  is introduced. Initial ply thickness is set to 0.4 mm, instead of averaged value 0.3 mm used in previous simulation approach. Transverse shear stiffness values are set to provide low-stiffness bending of the fabric comparable to cantilever test results.

Table 5. Continuum shell parameter

Parameter in MPa			
Thickness modulus	$E_{33} = 5.0$		
Transverse shear stiffness	$\kappa_{11} = 1.0$	$\kappa_{12} = 0.0$	$\kappa_{22} = 1.0$

Fig. 9 provides an exemplary simulation result using the CS approach. As suspected, a local compaction in thickness direction can now be accounted for by the modelling approach, which enables prediction of the local fiber volume content of the fabric stack between the metal sheets.

Moreover, a distinct difference is predicted for the fabrics shape beneath and beyond the metal sheet during molding. The fabric begins to wrinkle outside the contact areas created by the

sheets, which corresponds to the experimental observations. Furthermore, the influence of the blank holder forces can be represented in a more suitable way, since increased membrane forces lead to a local decrease of the layer thickness near edges. In the meantime, the hitherto existing prediction capabilities of the modelling approach, namely prediction of fiber orientations and plastification of the metal sheets, remain unchanged. Since reduced integrated CS elements with three integration points in thickness direction are sufficient, the numerical effort for the model does not increase compared to the original approach using stacked membrane and shell elements.

In summary, the usage of CS elements provides a variety of advantages and significantly improves the level of detail of the simulation without requiring additional numerical effort. However, this approach may only be used if the bending behavior of the fabric is of minor importance within the considered process, or if membrane forces, introduced by additional blank holders, dominate the draping procedure itself.

6. Conclusion and outlook

In this study, forming of FML has been analyzed by modeling the plies by conventional shell elements and by continuum shell elements. The fabric shear, bending and compression stiffness were varied. It has been found, that one should consider the tension-compression anisotropy of the textile. Unsuitably high fiber compaction stiffnesses resulting in shear bands, as previously forming studies showed.

When compressive strains are applied to a fabric, the gapping between the rovings is reduced, which requires much less effort than straining a fiber or roving under tension. This effect can easily be accounted for within the FABRIC model by implementing low compression stiffness compared to high tension stiffness. For further investigations, the in-plane compaction stiffness should be measured to identify a suitable

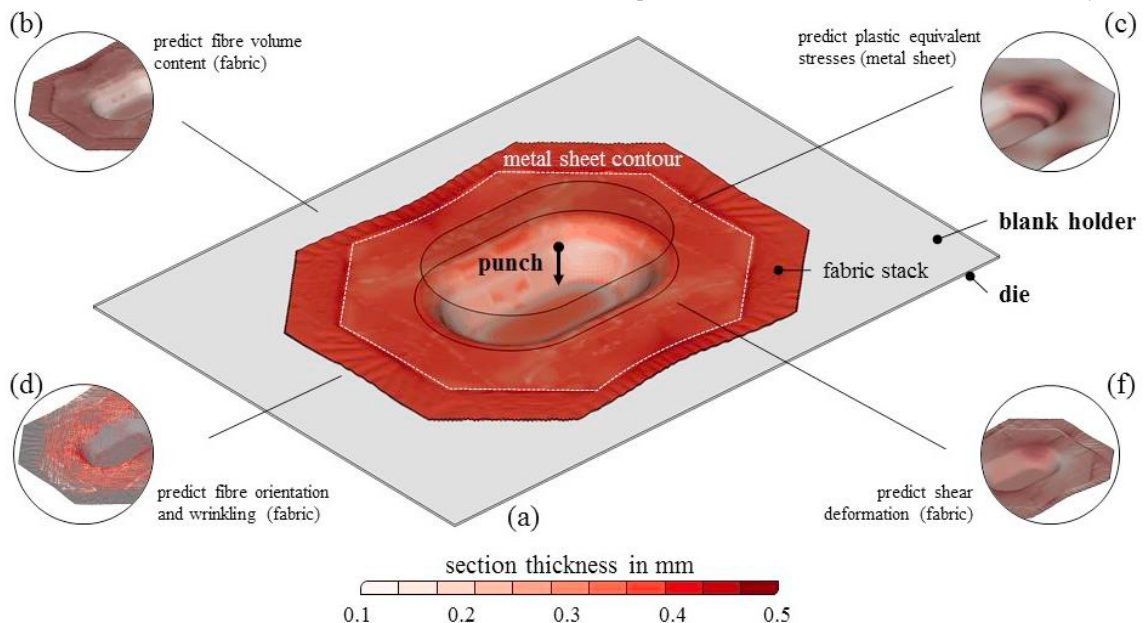


Fig. 9. (a) Prediction of the local section thickness within the fabric stack using continuum shell elements; (b-f) Prediction capabilities of the new process simulation approach.

value range. Therefore, an experimental setup has to be developed.

The bending stiffness of the fabric can be neglected, because it has no significant influence on the forming result between the metal sheets. The bending stiffness of the metal sheets dominates the forming behavior of the fabric and the fabric is therefore draped through kinematic constraints given by the stiff metal sheets. More important than the exact value of fabric bending, compression and shear stiffness is the ratio between the stiffnesses of these deformation modes.

An FML forming simulation approach based on continuum shell elements is promising, because thickness variations can be captured, which may lead to fracture of the metal sheets during experiments. In addition, the thickness variation allows a compaction of the fabric layers, which increases the fiber volume content and hinders the injection and infiltration of the matrix. Compaction of the fabric layers leads to higher contact stresses between fabric and metal sheet, which induces notches in the metal sheet and reduces formability of the metal sheet [15].

In current approaches, fluid propagation has been neglected. However, experimental trials prove a strong impact of the fluid pressure and viscosity on final part during processing. Consequently, future work will focus on the consideration of simultaneous fluid progression and under transient cavity pressure during molding. Given that the fluid propagation within the fabric is mainly determined by the local permeability, respectively its current deformation state (fiber volume content), compaction and local thickness variations ought to be predictable by the forming model. In this regard, the extension of the current approach, using continuum shell elements to account for compaction behavior, should provide a suitable framework. Poppe et al. [16] present a suitable approach for concurrent fluid progression during molding. However, its applicability to FML forming needs to be investigated.

### Acknowledgements

The German Research Foundation (DFG) kindly supports this research project (HE 6154/4-1, HE 6154/4-2). The authors would also like to thank the German State Ministry for Science, Research and Art of Baden-Württemberg (MWK) for funding the project “Forschungsbrücke Karlsruhe-Stuttgart” in which the continuum shell approach was developed. Moreover, the authors thank their colleagues for support, especially Constantin Krauß and Bastian Schäfer.

### References

- [1] Vlot A, Gunnink JW. *Fibre Metal Laminates: An Introduction*. Dordrecht: Springer Netherlands; 2001.
- [2] Botelho EC, Silva RA, Pardini LC, Rezende MC. A review on the development and properties of continuous fiber/epoxy/aluminum hybrid composites for aircraft structures. *Mat. Res.* 2006;9(3):247–56.
- [3] Sinke J. Manufacturing of GLARE Parts and Structures. *Applied Composite Materials* 2003;10(4/5):293–305.
- [4] Behrens B-A, Vucetic M, Neumann A, Osiecki T, Grbic N. Experimental Test and FEA of a Sheet Metal Forming Process of Composite Material and Steel Foil in Sandwich Design Using LS-DYNA. *KEM* 2015;651-653:439–45.
- [5] Behrens B-A, Hübner S, Neumann A. Forming Sheets of Metal and Fibre-reinforced Plastics to Hybrid Parts in One Deep Drawing Process. *Procedia Engineering* 2014;81:1608–13.
- [6] Wollmann T, Hahn M, Wiedemann S, Zeiser A, Jaschinski J, Modler N et al. Thermoplastic fibre metal laminates: Stiffness properties and forming behaviour by means of deep drawing. *Archives of Civil and Mechanical Engineering* 2018;18(2):442–50.
- [7] Rajabi A, Kadkhodayan M, Manoochehri M, Farjadfar R. Deep-drawing of thermoplastic metal-composite structures: Experimental investigations, statistical analyses and finite element modeling. *Journal of Materials Processing Technology* 2015;215:159–70.
- [8] Dau J, Lauter C, Damerow U, Homberg W, Tröster T. Multi-material systems for tailored automotive structural components. 18th international conference on composite materials 2011.
- [9] Engel B, Buhl J, Heftrich C. Modelling and Optimization of Lightweight-Sandwich-Sheets with an Adhesive Interlayer for the Forming Process Die Bending. *Procedia CIRP* 2014;18:168–73.
- [10] Mennecart T, Werner H, Ben Khalifa N, Weidenmann KA. Developments and Analyses of Alternative Processes for the Manufacturing of Fiber Metal Laminates.
- [11] Werner HO, Dörr D, Henning F, Kärger L. Numerical modeling of a hybrid forming process for three-dimensionally curved fiber-metal laminates. *AIP Conference Proceedings* 2019;2113(1):20019.
- [12] Dörr D, Brymerski W, Ropers S, Leutz D, Joppich T, Kärger L et al. A Benchmark Study of Finite Element Codes for Forming Simulation of Thermoplastic UD-Tapes. *Procedia CIRP* 2017;66:101–6.
- [13] Dörr D, Henning F, Kärger L. Nonlinear hyperviscoelastic modelling of intra-ply deformation behaviour in finite element forming simulation of continuously fibre-reinforced thermoplastics. *Composites Part A: Applied Science and Manufacturing* 2018;109:585–96.
- [14] Poppe C, Dörr D, Kraus F, Kärger L. Experimental and numerical investigation of the contact behavior during FE forming simulation of continuously reinforced composites in wet compression molding. *AIP Conference Proceedings* 2019;2113(1):20002.
- [15] Mennecart T, Gies S, Ben Khalifa N, Tekkaya AE. Analysis of the Influence of Fibers on the Formability of Metal Blanks in Manufacturing Processes for Fiber Metal Laminates. *JMMP* 2019;3(1):2.
- [16] Poppe C, Dörr D, Henning F, Kärger L. A 2D modeling approach for fluid propagation during FE-forming simulation of continuously reinforced composites in wet compression moulding. *AIP Conference Proceedings* 2018;1960(1):20022.